CHAPTER II
THEORETICAL BACKGROUND AND LITERATURE REVIEW

2.1 Electroactive Polymer (EAPs)

Electroactive polymers (EAPs) have emerged that visibly shape deformation can be produced. EAPs are receiving attention rapidly from scientists for a decade because of their high response to the external electric field. Generally, there are two essential forces that exhibit a volume or shape change, between repulsive intermolecular forces which act to expand the polymer network, and attractive forces that act to shrink it. Repulsive forces are usually electrostatic or hydrophobic in nature, whereas attraction is mediated by hydrogen bonding or van der Waals interactions. The competition between these counteracting forces, and hence the volume or shape change, can be controlled by subtle changes in parameters such as solvent, gel composition, temperature, pH, light, and etc (Bar-Cohen, 2002; Samatham *et al.*, 2007).

Electroactive polymers can be divided into two main groups: electronic EAPs and ionic EAPs. Electronic EAPs (electrostrictive, piezoelectric, electrostatic and ferroelectric materials) are the materials that perform the energy conversion between the electric and mechanical forms and hence can be utilized as both solid-state electromechanical actuators and motion sensors. High activation field is required to obtain the performance (approximately 200 MV/m). On the other hand, ionic EAPs (polymer gels, conductive polymers, carbon nanotubes and polymer-metal composites) which require low electric field strength (approximately 2 to 4 kV/m) are driven by diffusion of ions and they require an electrolyte for the actuation mechanism (Shahinpoor *et al.*, 2007).

Table 2.1 The comparison between electronic EAPs and ionic EAPs (Bar-cohen, 2002)

Electronic EAPs	Ionic EAPs
Electric elastomer EAP	Carbon nanotubes (CNT)
Electrostrictive graft elastomers	Conductive polymers (CPs)
Electrostrictive paper	Electrorheological fluids (ERF)
Electro-viscoelastic elastomer	Ionic polymer gels (IPG)
Ferroelectric polymers	Ionic polymer metallic composite
Liquid crystal elastomer (LCE)	(IPMC)

Electromechanical of a soft actuator from polyaniline particle and crosslinked poly (dimethyl siloxane) was fabricated by Hiamtup and coworkers (2006). Polyaniline (PANI) was synthesized via the oxidative coupling polymerization in an acid condition and de-doped in a solution of ammonia. The electrorheological (ER) properties of PANI/silicone oil suspensions were studied in oscillatory shear in the linear viscoelastic regime as the functions of electric field strength, particle concentration, and host fluid viscosity. They also investigated the switching characteristics of the ER response and confirmed the existence of residual gel structure when the field was switched off, if the applied stress was too small. The results showed that when the field was switched off a residual structure remained, whose yield stress increased with the strength of the applied field and particle concentration. When the applied stress exceeded the yield stress of the residual structure, a fast and fully reversible switching of the ER response was obtained.

An electroactive paper (EAPap) from cellulose (Phy Gel) was fabricated by Kunchornsup and his colleagues (2012). In this work, 1-butyl-3-methylimidazolium chloride ($BMIM^+Cl^-$), the well-known room temperature ionic liquid (RTIL) was applied to dissolve a micro-crystalline of the cellulose. The material was formed by solvent casting before the electromechanical properties including storage modulus response ($\Delta G'$), electrical sensitivity ($\Delta G'/G'_0$), and temporal response were investigated under the oscillatory shear mode as a function of the electric field strength from 0 to 1kV/mm and temperature. The actuation performance was

determined by a deflection experiment under applied electric field from 0 to 550 V/mm. The results showed that the storage moduli (G′) increase linearly under applied electric field at 333K. In addition, the storage moduli also increased in the presence of 1 kV/mm electric field but decreased when the temperature was above 313K which was attributed to the ionic association and the premature transition temperature. For the deflection experiment, the Phy gel bended to the positive electrode under 100 V/mm electric field which was due to the ionic and electronic polarization of $BMIM^+Cl^-$ and the functional group of the Phy Gel, hydroxyl group respectively. Furthermore, The Phy Gel showed the back and forth swinging due to the competitive effect between the movement of cation and anion in the Phy Gel under relatively high electric field strength, 525 to 550 V/mm.

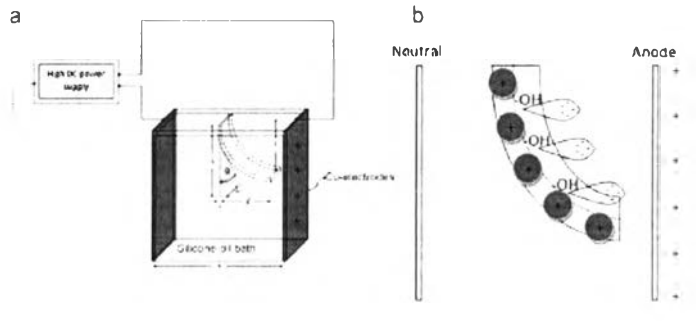

Figure 2.1 Schematic illustration of (a) bending response measurement of Phy gel suspended vertically in silicone-oil bath and sandwiched between copper electrodes and (b) actuation mechanism were from two dominating factors ; ionic polarization of $BMIM^+$ cation and electronic polarization of cellulosic hydroxyl group (Kunchornsup *et al.*, 2012).

Pure polyisoprene (PI) and polythiophene(PTh)/PI blends were produced and studied for electroactive applications (Puvanatvattana *et al.*, 2006). Electrorheological properties were determined under the oscillatory shear rate mode at various electric field strength from 0 to 2 kV/mm. PI was crosslinked by using dicumyl peroxide at various concentrations (crosslinking ratio of 2, 3, 5 and 7) to enhance mechanical properties. In case of pure PI, storage modulus (G′) increased while loss modulus (G″) decreased with increasing crosslinking ratio because of

changing from a fluid-like to a solid-like material. Maximum electrical sensitivity belonged to crosslinking ratio of 3 at 2 kV/mm electric field strength. Furthermore, 5, 10, 20 and 30 vol% of undoped PTh was embedded into the PI matrix. They found that the dynamic moduli increased with increasing the concentration of PTh, which can be explained by the polarization and induced dipole moments of both PI and PTh.

2.2 Shape Memory Materials

Shape memory materials (SMMs), including shape memory alloys (SMAs), shape memory polymers (SMPs) and shape memory composites (SMCs), have an ability to deform and recover their original shape when a particular stimulus is applied and subsequently removed. This behavior is well-known as a shape memory effect (SME) (Wei *et al.*, 1998). SMMs can be utilized for various applications, from biomedical devices (self-shrink suture and biocompatible actuator) (Small IV *et al.*, 2009; Yuan, 2010) to aerospace parts (deployable structure and morphing wings) (Fabrizio *et al.*, 2012).

In 1932, Gold-Cadmium (AuCd) as the first shape memory alloy (SMA). Later, Nickel-Titanium (NiTi), a significant recoverable and biocompatible shape memory alloy was discovered in 1971 which attracted the attention from the people. Today, a wide range of SMAs have been developed in solid, film and even foam shapes. Among them, only three alloy systems, namely NiTi-based, Cu-based (CuAlNi and CuZnAl) and Fe-based, are presently more of a commercial importance (Huang *et al.*, 2010). However, there are many drawbacks for SMA such as heaviness, low shape deformability and recoverability, and complexity in processing.

Shape memory polymers (SMPs) have been introduced in 1984 in Japan instead of SMAs to compensate their drawbacks (Meng *et al.*, 2009). SMPs are a family of smart materials that can be deformed into temporary shape and soon recover their original shape under a variety of external stimuli such as heat (Small IV *et al.*, 2009), light (Sodhi *et al.*, 2010), electricity (Jung *et al.*, 2010) and magnetic field (Brown *et al.*, 2007).

Table 2.2 The Comparison table between Shape Memory Polymer (SMP) vs. Shape Memory Alloys (SMA) (Olaru *et al.*, 2010)

Parameters	Shape Memory Polymer- SMP Vybormem	Shape Memory Alloys- NiTiX [6]
Density, g/cm³	0,8-1,2	6,3-6,7
Deformation, %	Up to 237	8
Young modulus T Ttrans, GPa	0,0088-1,0	72-98
Tensile strength, Yield, MPa	19,0	27,0
Temperature work , °C	(-15) / (+310)	(-50) /(+100)
Thermal conductivity, W/mK	0,12-0,35	12-18
Biocompatibility/degradability	Can be biocompatible and / or biodegradable	Good biocompatible and not biodegradable
Processing conditions	Low pressure, 250°C	High pressure, 1000°C
Corrosion resistance	Excellent	Very good
Costs	185€/kg	300-360€/kg
Hardness, Shore A	75	50-64
Compression set	72 hours @ 200°C	-

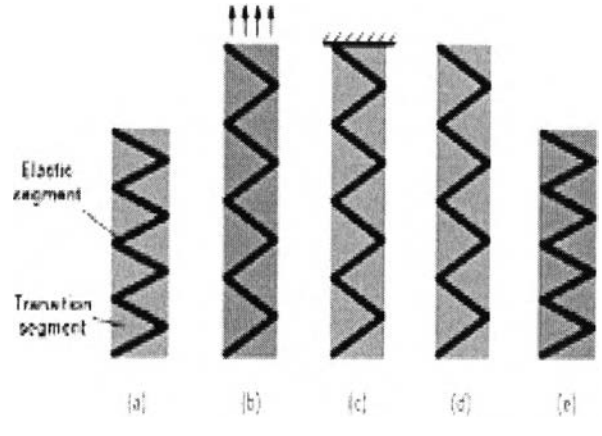

Figure 2.2 Illustration of the mechanism of the SME in thermo-responsive SMP: (a) hard at low temperature; (b) easily deformed at high temperature; (c) hard again after cooling; (d) temporary (deformed) shape after constraint removed; (e) shape recovery upon heating (Huang *et al.*, 2010).

Conventionally, a widely known shape memory polymer can be stimulated by heat. The mechanism of conventional SMPs usually consists of two main phases,

fixing phase or hard segment which can be crosslinked physically or chemically to give permanent shape. Another phase is reversible phase or soft segment which enable SMP to be programmed through applying stress while cooling down under transition temperature (T_{tran}) and recover by heating up above T_{tran} (Huang *et al.*, 2010).

Normally, high temperature above melting temperature is required to drive the shape recovery. However, the temperature is sometimes far from the normal body's temperature and sometimes even does harm to the organic tissue. Therefore, a key challenge is that a safer and more effective stimulus is necessary when SMPs are used as in vivo medical devices (Xiao *et al.*, 2010). Electroactive shape memory materials which are the materials that response to electricity, have been introduced later. These SMPs are always filled with electrical conductive fillers such as carbon nanotubes (CNTs), carbon particles, carbon fibers, nickel zinc ferrite ferromagnetic particles, conductive polymers, to enhance the electrical conductivity of the material (Gunes *et al.*, 2009; Petit *et al.*, 2008; Jung *et al.*, 2010; Runge *et al.*, 2010; Liu *et al.*, 2009). Also the hybrid system can be deployed to synergize the electroactive property of the material (Sahoo *et al.*, 2006).

2.3 Conductive polymers

Conductive polymers are organic materials which are composed of carbon and hydrogen atoms, or sometime heteroatoms such as nitrogen and sulfur are available in a polymer backbone (Kaynak, 1997). Conductive polymers was first discovered in 1960s by Heeger, Shirakawa and MacDiarmid, who successfully produced conducting doped polyacetylene with bromine and iodine vapor (Harun *et al.*, 2007).The structure of conductive polymer is an alternative single bond and double bonded sp^2 hybridized atoms, called conjugated double bond that π-electrons can delocalize along the polymer chain (Guimard *et al.*, 2007). Polyacetylene (PAC), Polyphenylene, and its derivatives; poly(p-phenylene vinyline) (PPV), poly(p-phenylene sulfide) (PPS), poly(p-phenylene oxide) (PPO) polypyrrole (PPY), polythiophenes (PThs), and polyanilene (PANI), are well-known conductive polymers.

polythiophenes (PThs), and polyanilene (PANI), are well-known conductive polymers.

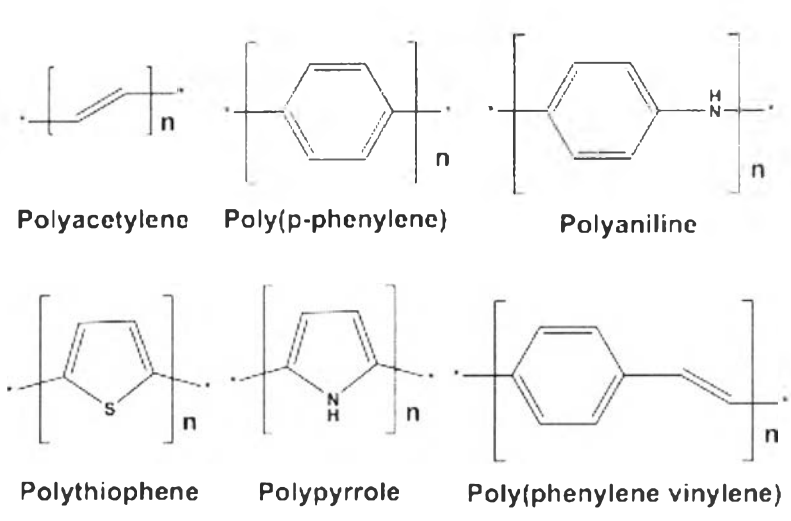

Figure 2.3 Conductive polymers (Choi *et al.*, 2008).

Conductivity of conductive polymers can be explained by the band theory (Pratt, 1996). Valence band (VB) or highest occupied molecular orbital (HOMO), Conduction band (CB) or lowest unoccupied molecular orbital (LUMO) and the band gap between VB and CB are important factor for the electron or hole conduction.

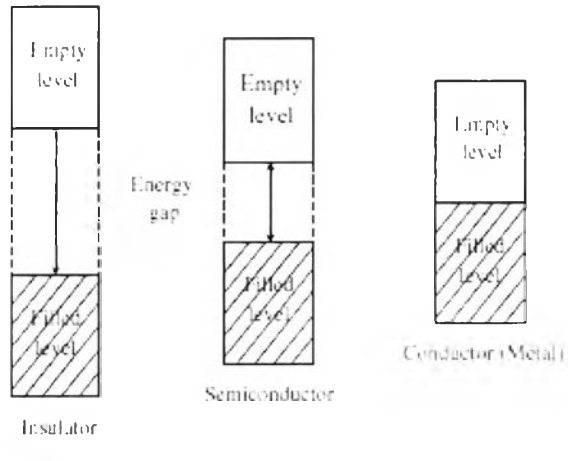

Figure 2.4 Electronic bands in solids (Park *et al.*, 2005).

2.4 Doping on conductive polymers

Generally, conductivity of conductive polymers are in the range of an insulator (conductivity is less than 10^{-7} S/cm) which have a large band gap (more than 1.5 eV) (Brédas et al., 1985). Doping with a weak oxidizing agent or a reducing agent results a reduction of a band gap. According to this reason, less energy required to stimulating an electron or a hole to jump over from the valence band to the conduction band and an insulator can become a semiconductor or conductor (Bonagamba *et al.*, 1995)

There are 2 distinct types for conductive polymer doping process. First, p-doping is a partial oxidation on the polymer backbone with oxidizing agent such as halogen (bromine and iodine), arsenic pentafluoride (AsF_5), iron(III) chloride, antimony pentachloride ($SbCl_5$), and etc. These are electron acceptors that withdraw electrons from conductive polymers in which positive solitons can be generated. In the opposite, n-type doping, reducing agent such as potassium ion (K^+) or sodium ion (Na^+). These are electron donors that donate electrons to conductive polymers to generate negative solitons on the polymer backbone (Hérold *et al.*, 1990; MacDiarmid, 2001; Pratt, 1996). Normally, after a doping process, the conductivity of polymers increases dramatically, as shown in figure 2.5.

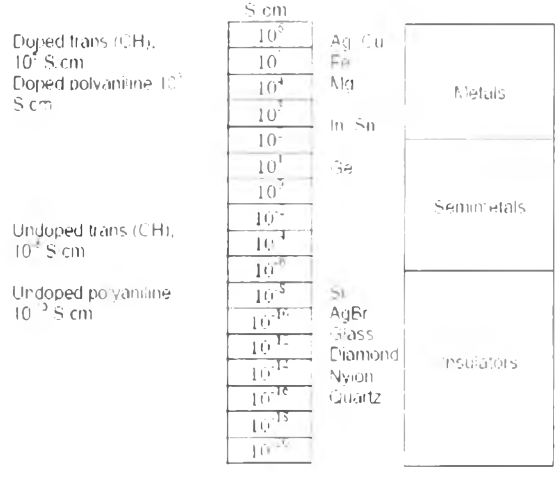

Figure 2.5 The conductivity before and after doping process of conductive polymer (polyacetylene and polyaniline) and other materials (Harun *et al.*, 2007).

A doping process produces a free radical and spin less charges which are couple with each other via a local resonance. This combination of these spin less charges and a free radical is called polaron, which a new localized electronic state has been created and diminish a band gap, respectively. Polarons will be replaced with bipolarons and bipolaron bands if doping is continued and a band gap becomes smaller. In case of heavily doping, the upper and lower bipolaron bands can be merged with CB and VB to produce the metallic conduction.

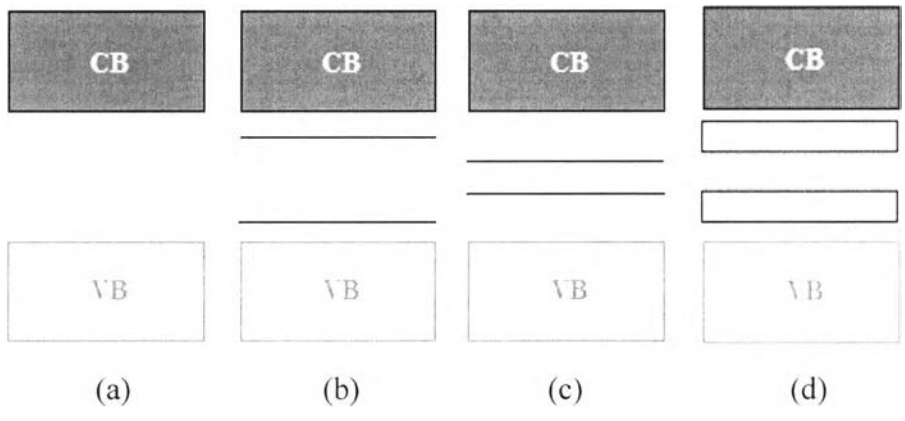

Figure 2.6 Electronic band in (a) neutral, (b) polaron, (c) bipolaron and (d) bipolaron band form of conductive polymers (Pratt, 1996).

Doping without reducing stability is a considerable criterion. A smaller band gap is considered to favor electrical conductivity.

There are two types of stability for conductive polymers. First, they have an extrinsic stability which is related to environmental agents such as oxygen, water, and peroxide. These agents will damage a polymer through nucleophilic, electrophilic, and free radical reactions. Stable coating is required to protect extrinsic unstable conductive polymers. Second, conductive polymers have an intrinsic stability so even in dry, oxygen free environment, degradation is still occurring over time. Intrinsic stability comes from an irreversible chemical reaction between a charged site of the polymer and thermally driven mechanism which can cause the polymer to lose its dopant.

2.5 Poly(p-phenylene) (PPP)

Polyparaphenylene (Poly(p-phenylene) or PPP) is one of the most ordinary conductive polymers, has been attracting some attentions for its high thermal stability and versatile electron structures achieved via different preparation technologies. Versatile synthetic routes of PPP were reported, which included the radical polymerization and typical organic chemistry procedures. Among these methods, one successful polymerization route studied widely is the bulk polymerization of benzene using aluminum chloride-copper (II) chloride system (Li *et al.*, 2008).

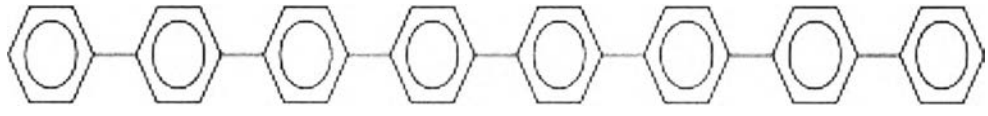

Figure 2.7 Polyparaphenylene (PPP) in neutral form (Bouzakraoui *et al.*, 2005).

Usually, PPP can enhance conductivity by doping with oxidizing agents such as arsenic pentafluoride (AsF_5), iron(III) chloride ($FeCl_3$) or sulfuric acid via p-type doping (Kunanuruksapong *et al.*, 2006) or reducing agents such as Li^+ or K^+ via n-type doping (Hérold *et al.*, 1990). Upon doping, a conductive polymer system with a net charge of zero is produced due to the close association of the counter ions with the charged conductive polymer backbone. This process introduces charge carriers, in the form of charged polarons or bipolarons (Guimard *et al.*, 2007).

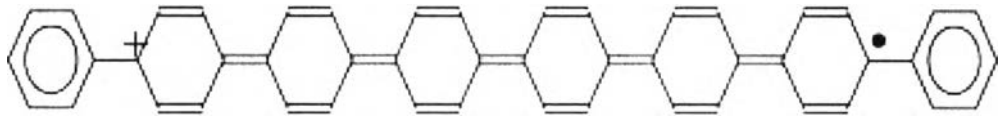

(a)

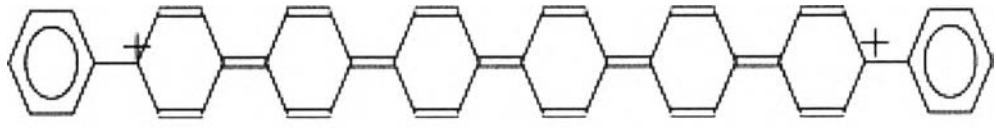

(b)

Figure 2.8 Polyparaphenylene (PPP) in (a) polaron and (b) bipolaron form (Bouzakraoui *et al.*, 2005).

PPP/zeolite composite was fabricated as a sensor for these following gases, CO_2, H_2, and NH_3 (Phumman *et al.*, 2009). First, PPP was synthesized via the oxidative polymerization due to the reaction between benzene, anhydrous aluminium choride ($AlCl_3$) and anhydrous cupric chloride ($CuCl_2$) at a mole ratio of 8:2:1 and at 32-37°C under N_2 atmosphere for 3 hours. Filtration with 18% Hydrochloric acid and distilled water was required. After that, undoped PPP (uPPP) particle was dried at 110°C for 3 hours before doped with $FeCl_3$-ethanol solution at a mole ratio of 50:1. Doped PPP (dPPP) was filtered and dried for 12 hours at room temperature. The infrared spectrum showed a very intense band at 805 cm^{-1} and moderate intense band at 999, 1396, and 1479 cm^{-1} which indicated the para aromatic substitution for synthesized undoped PPP. Peaks occurred at 763 and 695 cm^{-1} for the mono substitution and at 1545 and 1180 cm^{-1} for the intrinsic vibration of the polymer chain in the dope state. UV-VIS spectra showed the reflectance peak at 350 nm and about 300-400 nm for the π-π^* transition of the benzoid ring of uPPP and for 50:1 dPPP, respectively. From the thermogravimatric analysis, thermogram of uPPP and 50:1 dPPP displayed single step decompositions at 595 and 480°C respectively. DPPP had a lower decomposition temperature because of the defects in the polymer chain after doping. XRD pattern showed that the most intense d-spacing peak at 4.53 Å which is related to the length of the phenyl unit. After doping process, this peak represented a decrease in crystallinity.

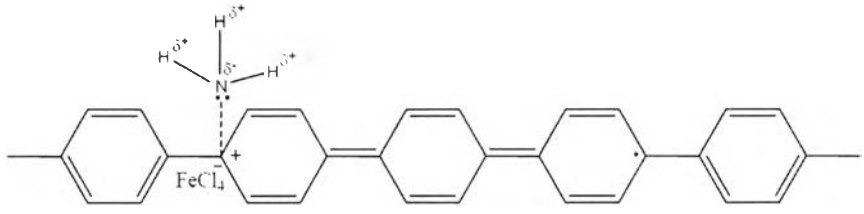

Figure 2.9 Proposed interaction between 50:1 dPPP and NH_3.

Plocharski et al., (2000) also reported that synthesized amorphous PPP can be doped by iron (III) ($FeCl_3$) chloride where conductivity was in the range of 10^{-8} to 10^{-5} S/cm. In addition, annealing the undoped amorphous PPP brought about a partially crystalline polymer before doping with $FeCl_3$ that enhanced the electrical conductivity by one order of magnitude. First, PPP was synthesized by the oxidative polymerization between benzene, aluminium choride ($AlCl_3$) and cupric chloride ($CuCl_2$) followed by below equation. The reaction was kept at 61°C for 60 hours.

$$nC_6H_6 + n/2O_2 \xrightarrow{AlCl_3,\ Cu_2Cl_2} (C_6H_4)_n + nH_2O. \qquad \text{(II-1)}$$

This obtained amorphous light brown undoped PPP (uPPP) was finally dried at 100-110°C in air for a day. Annealing for obtaining crystalline PPP was required for increasing conductivity. The amorphous uPPP was annealed in vacuum at 450°C for 4.5 hours. Obtained crystalline uPPP was determined by the different pattern in XRD measurement.

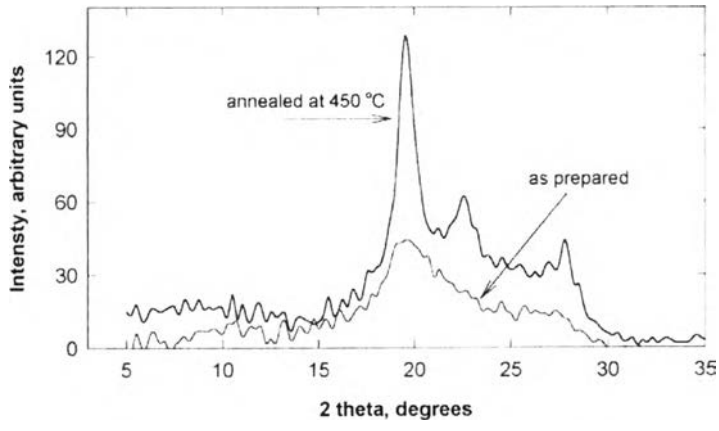

Figure 2.10 X-ray diffraction patterns for obtained amorphous uPPP and crystalline uPPP annealed at 450°C for 4.5 h in vacuum, Cu Ka radiation.

For PPP doping, 6 g of dried uPPP powder in 100 ml of distilled dry nitromethane was prepared in a flask. Then 0.3-3 g of anhydrous $FeCl_3$ dissolved in 80 ml nitromethane was added. Nitromethane solution of $FeCl_3$ resulted in the creation of $FeCl^-_4$ counterions which stabilized positive charges located at conjugated polymer chains. The mixture was stirred for a few hours. The doped PPP was then filtered out and washed in a funnel with 50 ml of fresh nitromethane. The powder was dried in air at 60–70°C for 12 hours. The concentration of iron was determined by a chemical analysis or/and X-ray fluorescence. The results showed that the conductivity of PPP increased with increasing concentration of iron and temperature. Furthermore, the electronic conductivities of the crystalline samples were more than one order of magnitude greater than their amorphous counterparts with the same doping level. Both types of dPPP have higher dielectric constants when the concentration of iron increased.

Kunanuruksapong and his coworkers (2007) reported that PPP can be synthesized via the Kovacic method by using benzene, aluminium choride ($AlCl_3$) and cupric chloride ($CuCl_2$) with the mole ratio of 1:0.5:0.5. The reaction was in 3-neck flask at 35-37°C for 3 hours. Then, the solution was cooled to 5°C and filtered with 18% hydrochloric acid and finally in hot distilled water until the washing had a pH of 7.0. At last, undoped PPP (uPPP) powder was dried at 27°C for 12 hours in

vacuum. Dried uPPP, which was a light brown solid powder, was obtained. Doped PPP (dPPP) can be prepared by the doping process with sulfuric acid (H_2SO_4) in a sealed flask under N_2 atmosphere. The mixture was stirred at 5°C for 2 hours. DPPP was filtered and dried at 27°C under vacuum for 12 hours. Dark brown powder was obtained. The higher degree of doping, the darker of brown color of dPPP powder. FTIR spectra of uPPP had characteristic peaks at 3025-3020, 1477, 1000, 805, 757 and 693 cm^{-1} which can be assigned to the C-H stretching of benzene ring, the double sides para-substitute stretching of benzene, the C-C stretching of benzene ring and the single side para-substitute stretching respectively. For dPPP, peaks occurred at 1530, 1080 and 810 cm^{-1} can be assigned to the double side para-substitute strectching of benzene ring and the C-C stretching of benzene ring after doping respectively. Peaks at 1477 and 805 cm^{-1} also shifted higher after the doping process. A degradation peak from the TGA thermogram of uPPP occurred at 700°C corresponding to the backbone degradation. For highly dPPP, peaks occurred at 220°C and 700°C corresponding to to the short chain and the long chain degradations, respectively. For the XRD pattern, peaks of uPPP at 2θ were equal to 19.58, 22.48, and 27.94, with corresponding *d-spacings* of 4.5301, 3.9518, and 3.1907 A, respectively. After doping, no new peaks detected but the peaks shifted to the higher 2θ and the intensity decreased. The specific conductivity of the obtained uPPP was 5.28×10^{-6} S/cm with a standard deviation of 4.86×10^{-7} S/cm and conductivity increased with increasing degree of doping.

2.6 Poly(ε-caprolactone)

Poly(ε-caprolactone) or PCL is a hydrophobic, semi-crystaline and biodegradable polyester which has a low melting and crystallization temperature (59-64°C and around -60°C respectively). PCL can be prepared by the ring-opening polymerization of the cyclic monomer ε-caprolactone via using stannous octoate ($Sn(Oct)_2$) as a catalyst (Colwell, 2006).

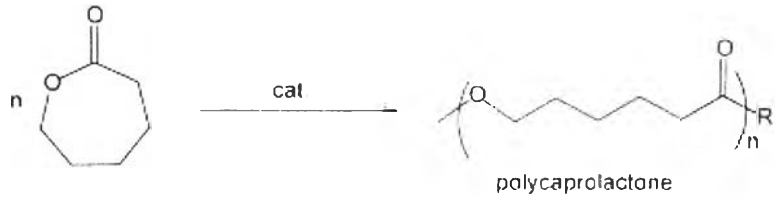

Figure 2.11 Synthesis of PCL (Majoumo-Mbe *et al.*, 2005).

There are several mechanisms for the polymerization of PCL: s anionic, cationic, co-ordination and radical. Each method affects the resulting molecular weight, molecular weight distribution, end group composition and chemical structure of the copolymers. PCL is soluble in chloroform, dichloromethane, carbon tetrachloride, benzene, toluene, cyclohexanone and 2-nitropropane at room temperature. Also PCL can be blended with polymers such as cellulose propionate, cellulose acetate butyrate, polylactic acid and polylactic acid-co-glycolic acid to improve stress crack resistance, dye ability and adhesion (Woodruff *et al.*, 2010).

At present, PCL is an alternative choice for producing electroactive material because of high flexibility and recoverability. Furthermore, the specific properties such as thermal or mechanical properties can be enhanced by crosslinking, blending and making composites with other polymers or fillers (Rabani *et al.*, 2006, Ping *et al.*, 2005, Lee *et al.*, 2008, Ajili *et al.*, 2009).

2.7 Crosslinking of Poly(ε-caprolactone)

Normally, PCL has many drawbacks such as low melting temperature and low elasticity. Therefore crosslinking is an essential procedure to enhance the thermal and mechanical properties (Mo-Ling, 1999). PCL can be crosslinked by two well-known methods, irradithe ation crosslinking (Zhu *et al.*, 2005; Darwis *et al.*, 1997) and the radical crosslinking via peroxide such as dicumyl peroxide (DCP) and benzoyl peroxide (BPO) (Pandini *et al.*, 2012; Han *et al.*, 2007).

(a) (b)

Figure 2.12 Chemical structures of: (a) benzoyl peroxide (BPO); and (b) dicumyl peroxide (DCP), widespread using peroxides for PCL crosslinking.

For the mechanism of crosslinking, free radical sites can be generated by both of the bombardment of high energetic radiation and peroxides, as shown on this following figure.

Initiation : $R\text{-}O\text{-}O\text{-}R \longrightarrow R\text{-}O\cdot$

Propagation : $R\text{-}O\cdot + CH_2\text{-}CH_2 \longrightarrow -CH\text{-}CH_2\text{-}$ or

$-CH_2\text{-}CH_2- \longrightarrow -CH\text{-}CH_2-$

Termination : $-CH\text{-}CH_2- + -CH\text{-}CH_2- \longrightarrow$ $-\underset{\displaystyle -CH\text{-}CH_2-}{\overset{|}{C}H\text{-}CH_2-}$

Figure 2.13 An initiation, propagation and termination step of crosslinking system with peroxides and the radiation (Mo-Ling, 1999).

Usually, there is a competitive effect about crosslinking and chain scission (fragmentation) in both of irradiation and peroxide crosslinking. However, peroxides attack polymer chains in a nearly random pattern so C-H, C-C and C-O bonds can possibly be attacked by peroxides. The C-H scission generates alkyl radicals, which cause crosslinking. For other chain scission including C-O bonds, the product of

scission are chain fragment capped by the carbonyl or carboxyl groups which are stabilized by the emission of CO and CO_2 (Mo-Ling, 1999).

Pandini et al., (2012) studied two-way thermo-responsive shape memory behavior which recovered more completely and compared with the one-way shape memory behavior by using semi-crystalline linear, three-arm and four-arm star methacrylate end-group PCL (assigned as PCL-L, PCL-T and PCL-F respectively). All type of PCL was crosslinked by using 2 wt% dicumyl peroxide (DCP) as a radical initiator. PCL were heated up to 80°C and held on for a while for eliminating air bubble then increase temperature to 115°C as curing temperature for 5 hours. Degree of crosslinking was measured by the degree of swelling and crosslinking density. Thermal mechanical properties and the two-way shape memory behavior of all kind of PCL were investigated employing a proper thermo-mechanical cycle, carried out by means of a dynamic mechanical analyzer. The results indicated that PCL-L was the densest polymer, which had a maximum degree of crosslinking. However, all of these materials showed the two-way shape memory behavior that strongly depended on the applied load (250, 500, 700 and 1,000 kPa) under heating-cooling cycle and on the material crosslink density. PCL-T was the best for actuation performance while PCL-F was the best for recovery performance at any constant load.

Chang et al., (2010) prepared end-carboxylated telechelic PCL and epoxidized natural rubber (ENR) blends which formed a crosslinked structure via the interchain reaction at 180°C for 30 minutes. The variation of xPCL/ENR (80/20, 70/30, and 50/50 (w/w)) blends were prepared by a solution blending in chloroform at room temperature and were compression moulded into 1 mm thickness film. Also different molecular weights of PCL (xPCL-1.2k, xPCL-2.0k and xPCL-3.0k) were used. Gel content of the blend was measured by Soxhlet extraction with chloroform. Dynamic mechanical tests were measured by a dynamic mechanical analyzer (DMA) at 2°C/min heating rate from -100°C to 100°C. Thermal transition of the blend was determined by differential scanning calorimeter (DSC) with 10°C/min heating rate and -10°C cooling rate. The temporary shape for shape memory experiment was prepared by stretching at a constant draw rate between $T_1 = T_m + 20°C$ and $T_2 = T_c - 20°C$ and shape recovery was determined by a heating process at 2°C/min. The

wt% and the amount of each type of MWNTs was varied from 0 wt% to 10 wt%. Electrical conductivity was evaluated by a four-point probe . Surface morphology of the samples were observed by scanning electron microscope (SEM) with 20 kV accelerating voltage. All of the mechanical properties were measured by a universal testing machine. Storage modulus of the samples was determined by dynamic mechanical analyzer (DMA) at the heating rate of 3°C/min from 25°C to 80°C and at 1Hz frequency. Finally, electro-active shape memory effect was determined by using self-made equipment that constant voltage was applied to the samples. They found that the most suitable content of MWNT and the ratio between MWNT and BPO were 5 wt% and 0.6 wt% respectively. All samples displayed shape memory effect under both 55°C water and 50V applied voltage. PEG-M/cPCL shows the best distribution because of increasing of hydrophilicity of PEG to MWNT. According to this reason, PEG-M/cPCL had the strongest interfacial effect and cause more effective shape memory effect and electrical property.

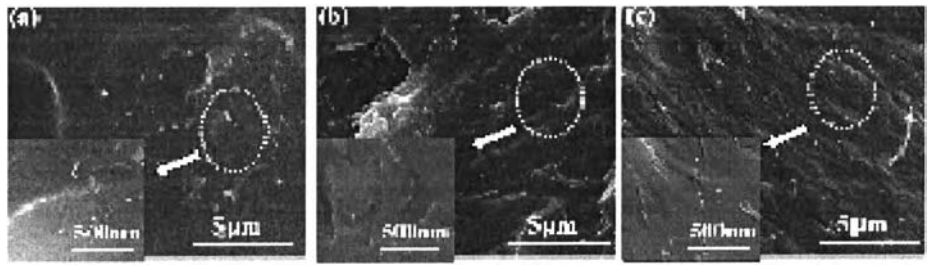

Figure 2.14 SEM images of the (a) cPCL/Raw-M, (b) cPCL/AO-M, and (c) cPCL/PEG-M with 5 wt % MWNTs and 3 wt % BPO (Xiao et al., 2010).

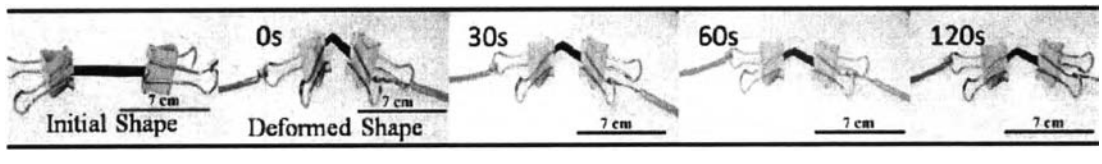

Figure 2.15 Self-made compliant electrode for shape memory effect experiment (Xiao et al., 2010).

ต้นฉบับ หน้าขาดหาย